

Differential glucose repression in common yeast strains in response to HXK2 deletion

Anne Kümmel¹, Jennifer Christina Ewald^{1,2,3}, Sarah-Maria Fendt^{1,2,3}, Stefan Jasper Jol^{1,3}, Paola Picotti¹, Ruedi Aebersold^{1,2,4,5}, Uwe Sauer^{1,2}, Nicola Zamboni^{1,2} & Matthias Heinemann^{1,2,6}

¹Institute of Molecular Systems Biology, ETH Zurich, Zurich, Switzerland; ²Competence Center for Systems Physiology and Metabolic Diseases, Zurich, Switzerland; ³Life Science Zurich PhD Program on Systems Biology of Complex Diseases, Zurich, Switzerland; ⁴Institute for Systems Biology, Seattle, WA, USA; ⁵Faculty of Science, University of Zurich, Zurich, Switzerland; and ⁶Molecular Systems Biology, Groningen Biomolecular Sciences and Biotechnology Institute, Groningen, The Netherlands

Correspondence: Matthias Heinemann, Institute of Molecular Systems Biology, ETH Zurich, Wolfgang-Pauli-Str. 16, Zurich 8093, Switzerland. Tel.: +41 44 6326366; fax: +41 44 6331051; e-mail: heinemann@imsb.biol.ethz.ch

Present address: Anne Kümmel, Novartis Institutes for BioMedical Research, Basel, Switzerland.

Received 17 July 2009; revised 4 January 2010; accepted 18 January 2010.
Final version published online 24 March 2010.

DOI:10.1111/j.1567-1364.2010.00609.x

Editor: Hyun Ah Kang

Keywords

glucose repression; hexokinase 2; FY4; CEN.PK; PKA; metabolomics.

Introduction

Under high glucose conditions and despite the presence of oxygen, the yeast *Saccharomyces cerevisiae* shows an almost exclusively fermentative metabolism, which is characterized by excretion of ethanol and absence of respiratory activity (Carlson, 1999; Rolland *et al.*, 2002). This effect is called catabolite or glucose repression and is reminiscent of the Warburg effect that occurs in several tumor cells (Johnston & Kim, 2005). Next to the distinct physiology, invertase (SUC2) expression/activity is also frequently used in the field as a reporter for the state of glucose repression.

Glucose repression in yeast is primarily realized by the Hxk2/Snf1 pathway (Gancedo, 1998; Rolland *et al.*, 2002). Although many molecular details of this pathway have been elucidated, a holistic understanding of its complete func-

Abstract

Under aerobic, high glucose conditions, *Saccharomyces cerevisiae* exhibits glucose repression and thus a predominantly fermentative metabolism. Here, we show that two commonly used prototrophic representatives of the CEN.PK and S288C strain families respond differently to deletion of the hexokinase 2 (HXK2) – a key player in glucose repression: In CEN.PK, growth rate collapses and derepression occurs on the physiological level, while the S288C descendant FY4 Δ hxk2 still grows like the parent strain and shows a fully repressed metabolism. A CEN.PK Δ hxk2 strain with a repaired adenylate cyclase gene CYR1 maintains repression but not growth rate. A comparison of the parent strain's physiology, metabolome, and proteome revealed higher metabolic rates, identical biomass, and byproduct yields, suggesting a lower Snf1 activity and a higher protein kinase A (PKA) activity in CEN.PK. This study highlights the importance of the genetic background in the processes of glucose signaling and regulation, contributes novel evidence on the overlap between the classical glucose repression pathway and the cAMP/PKA signaling pathway, and might have the potential to resolve some of the conflicting findings existing in the field.

tioning still remains elusive (Bisson & Kunathigan, 2003). It is clear, however, that the glucose phosphorylating enzyme hexokinase 2 (Hxk2) has a pivotal regulatory role (Randez-Gil *et al.*, 1998; de la Cera *et al.*, 2002; Ahuatzí *et al.*, 2004, 2007). There are certain indications that the glycolytic flux might be the signal that determines the degree of glucose repression (Jiang *et al.*, 2000; Elbing *et al.*, 2004; Otterstedt *et al.*, 2004). A classical experiment in the field of glucose repression is the deletion of Hxk2. Using auxotrophic strains, it was originally found that glucose repression is not active any more, as identified on the basis of increased SUC2 expression/activity (Zimmermann & Scheel, 1977; Entian, 1980; Ma & Botstein, 1986). Subsequent work, however, has shown that when Hxk2 is not present, hexokinase 1 (Hxk1) can also maintain glucose repression (Rose *et al.*, 1991; De Winde *et al.*, 1996).

Such conflicting findings with respect to the effect of HXK2 deletions on glucose repression can likely be explained by the fact that the used strains were not genetically identical. In some strains, the redundancy in the form of the Hxk1 isoenzyme might compensate for the loss of Hxk2. Alternatively, the cAMP/protein kinase A (PKA) pathway, which also has a role in regulating Snf1 (Hedbacker *et al.*, 2004; Slattery *et al.*, 2008), could realize an Hxk1/2-independent degree of glucose repression (Mbonyi *et al.*, 1990; Zaragoza *et al.*, 1999). Overall, conflicting findings such as those on the effect of HXK2 deletions with respect to glucose repression and the application of different means to assess glucose repression (i.e. SUC2 expression/activity vs. physiological quantification of glucose repression) hamper further progression in the field.

Focusing on the physiological manifestation of glucose repression, we carried out a comparative investigation of prototrophic representatives of two important yeast strain families that are frequently used to study glucose signaling and regulation and that show different responses to HXK2 deletions. The CEN.PK strain, a prominent yeast reference strain selected in a multilab effort (van Dijken *et al.*, 2000) shows on the physiological level a completely derepressed metabolism upon deletion of the HXK2 gene. In contrast, the FY4 strain (Winston *et al.*, 1995), a descendant of the first sequenced yeast strain and a prototrophic version of the strain BY strain with which most strain libraries were generated, fully retains physiologically the state of glucose repression when the same gene is deleted. A recent genome-wide analysis of nucleotide-level variations in *S. cerevisiae* strains has revealed that the FY4 strain, which is nearly identical to the BY4716 strain investigated in this analysis (Brachmann *et al.*, 1998), and the CEN.PK strain are rather similar. Genetic variation was found in only a small fraction of the genome (80% of the single nucleotide polymorphisms in CEN.PK in 18% of the genome), and only 17 genes in CEN.PK carry a whole or a partial (longer than 500 bps in size) deletion in comparison with BY4716 (with 41% of those genes not having an assigned biological function) (Schacherer *et al.*, 2007).

In this paper we set out to investigate the differences in these two strains under high glucose conditions. Specifically, we aimed at elucidating why these two strains respond differently on the physiological level to a deletion of the HXK2 gene and whether the known defect in the CYR1 gene (encoding adenylate cyclase, involved in cAMP synthesis) in CEN.PK (Vanhalewyn *et al.*, 1999) is responsible for the different behavior. We compare the physiology, metabolome, and proteome of the two yeast strains and a variant of one of them. We find significant differences between these strains, providing compelling evidence for the effect of the genetic background on major metabolic pathways such as those involved in glucose signaling in yeast. Furthermore,

our study provides support for an earlier hypothesized link between the classical glucose repression pathway and the glucose-activated cAMP/PKA signaling pathway.

Materials and methods

Strains and culture conditions

The strains used in this study are listed in Table 1. In CEN.PK JT4, the HXK2 gene was deleted by the short flanking homology method using the loxP-kanMX4-loxP gene disruption cassette (Guldener *et al.*, 1996). The deletion cassette was amplified from pUG6, using as a forward primer 5'-TCTTTGTTGCACCTTCGCCACTGTCTTATCTACAAAACACTTTCGTACGCTGCAGGTC-3', which includes 18 nucleotides complementary to pUG6 and a 40-nucleotide extension corresponding to the region -150 to -110 upstream of the start codon of the HXK2 ORF, and using as a reverse primer 5'-AGTACGCAAGCTATCTAGAGGAGGGTTAAATAGTGGATCTGATATCACCTA-3', which includes 21 nucleotides complementary to pUG6 and 40 nucleotides corresponding to the region +1851 to +1811 downstream of the start codon of the HXK2 ORF. Deletion of the HXK2 ORF was confirmed by PCR on genomic DNA extracted from G418R transformants.

In all experiments, cells were grown in minimal defined medium with glucose as sole carbon source. The medium was prepared from autoclaved salt and glucose solutions and sterile filtered solutions of vitamins and trace metals to reach concentrations as described in Verduyn *et al.* (1992). Liquid precultures with 10 g L⁻¹ glucose were inoculated by colonies from YPD plates. In all experiments, the glucose concentration was 10 g L⁻¹ and the temperature was maintained at 30 °C. Phthalate buffer (10 mM for shake flask experiments, 90 mM for ¹³C labeling experiments) was used to maintain the pH at value of 5.

Table 1. Yeast strains used in this work

Strain	Relevant genotype	Source or reference
CEN.PK 113-7D	<i>MATa</i>	Euroscarf (van Dijken <i>et al.</i> , 2000)
CEN.PK Δ <i>hxx2</i>	CEN.PK 113-7D <i>hxx2::kanMX4</i>	Blank & Sauer (2004)
CEN.PK JT4	<i>MATa</i> LCR1	M. Luttkik (pers. commun.)
CEN.PK JT4 Δ <i>hxx2</i>	CEN.PK JT4 <i>hxx2::kanMX4</i>	This study
FY4	<i>MATa</i>	Winston <i>et al.</i> (1995)
FY4 Δ <i>hxx2</i>	FY4 <i>hxx2::kanMX4</i>	C. Boone (pers. commun.)

Sequencing of HXK2 gene

The HXK2 gene was amplified by PCR from the FY4 and CEN.PK genome using a primers pair (5'-CTTTGAAAAG GTTGTAGGAA-3' and 5'-TAGAAAAAGGGCACCTTC TT-3') to amplify a 1571-bp region containing the gene. The resulting PCR product was cleaned with the QIAquick PCR Purification kit (Qiagen, Valencia, CA), and was sent to Microsynth AG (Balgach, Switzerland) for sequencing with the PCR primers and two internal primers (5'-ATATCG GAACAAACATCGTA-3' and 5'-TACTACTGACCCAGAAA CTAA-3'). The resulting four sequenced fragments were aligned and compared with the YGL253W gene from the *Saccharomyces* Genome Database (Tettelin *et al.*, 1997).

Biomass and extracellular metabolite concentrations

Biomass concentrations were monitored by measuring $OD_{600\text{ nm}}$ with a spectrophotometer (Pharmacia Novaspec II). The biomass dry weight (DW) was calculated using an earlier determined OD-to-biomass DW correlation coefficient of $0.486 \frac{\text{gDW/l}}{\text{OD}}$ for FY4 and $0.52 \frac{\text{gDW/l}}{\text{OD}}$ for CEN.PK strains. To determine the extracellular concentrations of glucose, ethanol, acetate, pyruvate, and glycerol, 1-mL samples were taken and centrifuged for 4 min at 2250 g at 4 °C. Unless otherwise noted, the supernatant was analyzed with an HPLC system (HP1100, Agilent Technologies), equipped with a polymer column (Aminex HPX-87, BioRad). As eluent, 5 mM H_2SO_4 was used and the column was heated to 60 °C. The compounds were detected and quantified with a refractive index (RI) detector and an UV/Vis-detector (DAD). For absolute quantification, calibration curves with external standards for the corresponding pure substance obtained from Sigma were used. Growth rates, μ , and biomass yields, $Y_{\frac{x}{s}}$, were calculated by linear regression (MATLAB, function *regress.m*) using the following equations, respectively:

$$\ln(x) = \ln(x_0) + \mu t \quad (1)$$

$$x = x_0 + Y_{\frac{x}{s}}(c_{\text{glc}_0} - c_{\text{glc}}) \quad (2)$$

based on the biomass concentrations, x , and extracellular glucose concentrations, c_{glc} , obtained from all biological replicates. The yields of ethanol, acetate, glycerol, and pyruvate were calculated using equations analogous to Eqn. (2). The remaining uptake and production rates were determined from the estimated values.

Respiratory tricarboxylic acid (TCA) cycle activity

The respiratory TCA cycle activity was determined from ^{13}C -labeling experiments, where 20% of the glucose in the

medium was uniformly labeled ($\geq 99\%$ enrichment, obtained from Cambridge Isotope Labs). These experiments were carried out in deep well plates with a culture volume of 1.2 mL and the biomass concentration was measured at 600 nm (Spectra MAX Plus, Bucher Biotec AG). Cultures were harvested during exponential growth at ODs between 0.8 and 1.3 and centrifuged at 4 °C and 2250 g for 3 min. Supernatant and cell pellets were frozen separately at -40 °C. Extracellular metabolite concentrations in the supernatant were determined using HPLC-RI/DAD methods as described above.

To determine the labeling patterns in proteogenic amino acids, samples were prepared and analyzed by GC-MS. Cell pellets were hydrolyzed in 180 μL 6 M HCl at 105 °C for 12 h and the hydrolysate dried at 95 °C. The free amino acids were derivatized at 85 °C for 1 h using 20 μL dimethylformamide and 20 μL *N*-(tert-butyltrimethylsilyl)-*N*-methyltrifluoroacetamide+1% tert-butyltrimethylchlorosilane. GC-MS analysis was carried out using a GC (series 6890N, Agilent Technologies) in combination with a mass spectrometer (5973, Agilent Technologies) (Fischer *et al.*, 2004). The respiratory TCA cycle activity was calculated from the fraction of mitochondrial oxaloacetate from anaplerosis, which was calculated from ^{13}C -labeling patterns using FiatFlux (Zamboni *et al.*, 2005).

Intracellular metabolite concentrations

Intracellular metabolite concentrations of two biological and two technical replicates were determined from samples withdrawn from culture at an OD of approximately 1.5. To quench metabolism and extract intracellular metabolites, the following procedure was used (adapted from de Koning & van Dam, 1992; Gonzalez *et al.*, 1997). Samples of 1–4 mL were taken at each sampling time point and quenched in methanol at -40 °C. For the determination of the cAMP concentrations, a sample volume of 10 mL was taken. After centrifuging for 3 min at 15 550 g in a rotor precooled to -9 °C, the samples were frozen at -40 °C. Intracellular metabolites were extracted by incubation in 75% ethanol for 3 min at 95 °C. The supernatant was collected after centrifuging in a precooled rotor (-9 °C).

For quantification by GC-TOF, two sample aliquots were derivatized with either TMS-agent [*N*-methyl-*N*-(trimethylsilyl) trifluoroacetamide, Fluka] or TBDMS agent (*N*-tert-butyltrimethylsilyl-*N*-methyltrifluoroacetamide, Fluka). The samples were separated via GC on an HP5-MS column (Hewlett-Packard, length 30 m \times ID 0.25 \times film 0.25 μm) and injected for MS analysis into a TOF spectrometer (Pegasus III, Leco). Detailed information on process parameters are described in Ewald *et al.* (2009). Leco CHROMATOF software (version 2.32) was used for acquisition. An auto-sampler (MPS2, Gerstel) controlled by Gerstel MAESTRO

software was used to derivatize samples just-in-time before injection to the GC-TOF system.

For quantification by LC-MS/MS, an ion-pairing reverse phase LC method was adapted from Luo *et al.* (2007). The mobile phase was composed of eluent A (aqueous solution of 10 mM tributylamine and 15 mM acetic acid) and eluent B (methanol); the gradient profile was as follows: $t = 0$ min, 0% B; $t = 15$ min, 55% B; $t = 27$ min, 66% B; $t = 28$ min, 100% B. The end-capped C18 column (Synergi Hydro RP, 2.1×150 mm, $4 \mu\text{m}$ particles; Phenomenex) was used.

The column was equilibrated for 20 min before each injection: flow rate $200 \mu\text{L min}^{-1}$, column temperature controlled at 40°C ; injection volume $8 \mu\text{L}$. For tandem MS analysis, an Applied Biosystems/MDS Sciex 4000 QTRAP mass spectrometer [Applied Biosystems (AB)/MDS Sciex] was coupled to the LC. ANALYST software (version 1.4.2, AB/MDS Sciex) was used for acquisition and peak integration. All analyses were performed in negative mode and selected reaction-monitoring mode with Q1 and Q3 set to unit resolution. Ion spray voltage, auxiliary gas temperature, nebulizer gas, auxiliary gas, curtain gas, and collision gas were set to -4200 V, 650°C , 65, 40, 10, 4 (arbitrary units), respectively. Nitrogen (Pangas) was used as curtain and collision gas.

Decustering potential collision energy and collision cell exit potential were optimized separately for each compound. To obtain temporal resolution of 1 Hz or greater for each transition, the run was divided into five segments and the dwell time for each transition was set to 50 ms.

To calculate intracellular concentrations, we used a conversion factor of $2 \mu\text{L mg}^{-1} \text{CDW}$. SEs σ_m for the sample means m are estimated from the data and for display on logarithmic scale transformed according to error propagation based on the derivative method:

$$\sigma_{\log} = \frac{\partial \ln m}{\partial m} \sigma_m = \frac{\sigma_m}{m}$$

Protein abundances

To determine protein concentration, duplicate samples of 25 mL were harvested on ice and washed twice with 5 mL washing buffer (20 mM HEPES pH 7.5, 2 mM EDTA). During washing, the protein samples were centrifuged for 5 min at $3750g$ at 4°C and the supernatant discarded afterwards. Cell pellets were frozen at -80°C .

For protein extraction, the cell pellets were thawed and resuspended in an ice cold lysis buffer containing 20 mM TrisHCl pH 8.0, 2 mM dithiothreitol, 100 mM KCl, 10 mM EDTA, and complete yeast protease inhibitors cocktail (Roche), using 1 mL of lysis buffer per gram of yeast. Yeast cells were lysed by glass bead beating, and lysed cells were centrifuged to remove cellular debris. The supernatant was

transferred to a fresh tube and the protein concentration in the extract was determined by Bradford assay. Proteins were precipitated by adding six volumes of cold (-20°C) acetone and resolubilized in a digestion buffer containing 8 M urea and 0.1 M NH_4HCO_3 . A $100\text{-}\mu\text{g}$ protein aliquot of each yeast protein sample was transferred to a fresh tube and mixed with an equal amount of ^{15}N -labeled yeast proteins. To digest the proteins, they were reduced with 12 mM dithiothreitol for 30 min at 35°C and alkylated with 40 mM iodoacetamide for 45 min at 25°C , in the dark. Samples were diluted with 0.1 M NH_4HCO_3 to a final concentration of 1.5 M urea and sequencing grade porcine trypsin (Promega) was added to a final enzyme : substrate ratio of 1 : 100. The digestion was stopped by acidification with formic acid to a final pH < 3 . Peptide mixtures were cleaned on Sep-Pak tC18 cartridges (Waters) eluted with 60% acetonitrile. Peptides were evaporated on a vacuum centrifuge to dryness, resolubilized in 0.1% formic acid and immediately analyzed.

Protein abundances were determined by a selective/multiple reaction monitoring (S/MRM)-based MS approach as follows. For each target protein, a set of five proteotypic peptides preferentially observed in shotgun proteomics experiments (King *et al.*, 2006) or predicted to have suitable MS properties (Mallick *et al.*, 2007) was selected for S/MRM analysis. For each peptide, three to eight transitions were calculated, corresponding to fragment ions of the γ -series. Fragment ions with m/z above the precursor ion m/z were prioritized. The precursor/fragment ion transitions were used to detect by S/MRM the peptides of interest in whole *S. cerevisiae* protein digests and to trigger acquisition of the full fragment ion spectra of the peptides (S/MRM-triggered MS2), as previously described (Picotti *et al.*, 2008). Each SRM assay was validated by acquiring a full tandem mass spectrum of the corresponding peptide.

Samples were analyzed on a hybrid triple quadrupole/ion trap mass spectrometer (4000QTrap, AB/MDS-Sciex) equipped with a nanoelectrospray ion source. Chromatographic separations of peptides were performed on a Tempo nano LC system (Applied Biosystems) coupled to a 15-cm fused silica emitter, $75 \mu\text{m}$ diameter, packed with a Magic C18 AQ 5 mm resin (Michrom BioResources). Peptides were loaded on the column from a cooled (4°C) Tempo auto-sampler and separated with a linear gradient of acetonitrile/water, containing 0.1% formic acid, at a flow rate of 300 nL min^{-1} . A gradient from 5% to 30% acetonitrile in 30 or 60 min was used. The pipeline used to analyze MS2 data and extract the optimal coordinates for the S/MRM assays is described elsewhere (Picotti *et al.*, 2008).

For the quantitative analysis, a ^{15}N -labeled yeast digest was derived from a yeast batch culture that displayed diauxic growth on minimal medium with 20 g L^{-1} glucose and ^{15}N -labeled ammonium as nitrogen source. To obtain high

coverage of metabolic proteins, aliquots from the different phases (growth on glucose, transient phase, and growth on ethanol) of this experiment were mixed. The heavy labeled protein mixture was used as an internal standard and was spiked into each sample at a 1 : 1 ratio before digestion. The three most intense S/MRM transitions from each validated peptide and for the corresponding ^{15}N -labeled analogue were chosen for quantitative analysis. Quantitation was performed in scheduled-S/MRM mode (retention time window, 300 s; target scan time, 2.4 s), using the acquisition software ANALYST 1.5, beta version (AB/MDS Sciex). Peak height was determined with MULTIQUNT 1.0.0.1 software (AB/MDS Sciex) after confirming for each peptide the coelution of all six transitions. Peak height ratios of the sample transition and internal standard transition were used to corrected for spray efficiency and ionization differences between runs.

To calculate the average protein abundances from the two biological replicates, mean values of peptide amounts were calculated from the transitions, mean values for proteins from the peptide mean values, and finally the two biological replicates were averaged. A conservative estimation of the SD was calculated from the variance of the pool of all measured transitions for the respective protein.

Osmotic shock experiments

To determine the survival rate after hyperosmotic shock, we adapted a method reported in Beney *et al.* (2001). CFU for an aliquot of yeast culture exposed to hyperosmotic shock and a nontreated aliquot – both from an exponentially growing culture – were counted. For hyperosmotic shock treatment, an aliquot of 1 mL was mixed with 9 mL autoclaved glycerol/water solution (116.9 g glycerol in 50 mL water, approximately 65 MPa) and left for 40 min at room temperature. Both treated and nontreated samples were diluted 33 000 and 66 000 times, respectively, in autoclaved isotonic NaCl solution (9 g L^{-1}) and 200 μL spread on YPD plates. After 2 days of incubation at 30°C , photographs were taken and the CFU counted. The survival rate was calculated as the ratio of CFU of treated vs. nontreated samples.

Transcription factor (TF) analysis of protein abundances

TFs, which are associated more often than by chance with the subset of proteins that are three times less abundant in CEN.PK compared with FY4 were determined by a statistical enrichment analysis adopted from Boyle *et al.* (2004). We here applied the documented TF–gene associations reported by Teixeira *et al.* (2006). For each TF that has at least one interaction with any of the measured proteins, a *P*-value based on a hypergeometric distribution was calculated:

$$P_j = 1 - \sum_{i=0}^{k_j-1} \frac{\binom{M_j}{i} \binom{N-M_j}{n-i}}{\binom{N}{n}} \quad (3)$$

where N is the total number of proteins measured and n the number of proteins that are three times less abundant in CEN.PK; M_j and k_j are the number of measured proteins and the number of measured, three times less abundant proteins in CEN.PK, respectively, that interact with TF j . The *P*-value calculated in this way gives the probability that the TF has at least the observed number of interactions with the subset of less abundant proteins. Detailed results are provided in Supporting Information, Table S1.

Results

Between the two strains compared here, there is one known genetic difference that likely is relevant for glucose signaling and regulation: a point mutation in the CEN.PK CYR1 gene encoding the adenylate cyclase prevents this strain from showing the otherwise typical cAMP increase upon sudden glucose excess (Vanhalwyn *et al.*, 1999), thus in principle lacking the PKA pathway as an alternative means for glucose repression. To assess whether the lacking CYR1 activation in CEN.PK could be the reason for the different responses to an HXK2 deletion, we also analyzed a CEN.PK strain with repaired CYR1, called JT4. In all experiments, the strains were grown aerobically in batch mode on glucose minimal medium and samples were taken at high residual glucose concentrations.

Physiological comparison

First, we determined the physiology of the strains. Here, CEN.PK and JT4 are absolutely identical in terms of rates and yields (Table 2). This was also expected, as the point mutation in CYR1 impairs the glucose- and acidification-induced cAMP increase in derepressed cells, whereas glucose-repressed cells are usually thought not to be affected by this mutation (Vanhalwyn *et al.*, 1999). The FY4 strain, in contrast, shows a lower growth rate than the two CEN.PK strains (Table 2). The yields, however, are very similar in all strains (Table 2). Further, all strains show a physiologically fully repressed metabolism with practically absent respiratory TCA cycle activity as determined by ^{13}C metabolic flux analysis (Fig. 1). Overall, while the relative intracellular flux distribution is identical in all analyzed strains, the CEN.PK and the JT4 strains have much higher metabolic rates than the FY4 strain.

Significant differences occur when HXK2 is deleted. CEN.PK Δhxk2 shows a significantly reduced growth rate (0.22 h^{-1}) and a derepressed metabolism reaching a biomass yield of $0.43 \text{ g}_{\text{DW}} \text{ g}_{\text{glucose}}^{-1}$, which is comparable to fully

Table 2. Physiological parameters of aerobic glucose-growing batch cultures in shake flasks

Strain		Biomass	Glucose	Ethanol	Acetate	Glycerol	Pyruvate
		Yield ($\text{g g}_{\text{glc}}^{-1}$)					
CEN.PK	wt	0.114 ± 0.004	–	0.41 ± 0.02	0.011 ± 0.001	0.027 ± 0.002	0.0032 ± 0.0002
	JT4	0.107 ± 0.005	–	0.37 ± 0.02	0.008 ± 0.001	0.029 ± 0.002	0.0029 ± 0.0002
FY4	wt	0.113 ± 0.004	–	0.40 ± 0.03	0.008 ± 0.001	0.033 ± 0.004	0.0036 ± 0.0002
		Rates ($\text{g g}_{\text{DW}}^{-1} \text{h}^{-1}$)					
CEN.PK	wt	0.46 ± 0.005	4.04 ± 0.14	1.66 ± 0.10	0.044 ± 0.004	0.109 ± 0.009	0.013 ± 0.001
	JT4	0.45 ± 0.006	4.21 ± 0.20	1.55 ± 0.13	0.034 ± 0.005	0.122 ± 0.010	0.012 ± 0.001
FY4	wt	0.33 ± 0.009	2.92 ± 0.13	1.16 ± 0.11	0.023 ± 0.003	0.096 ± 0.013	0.011 ± 0.001

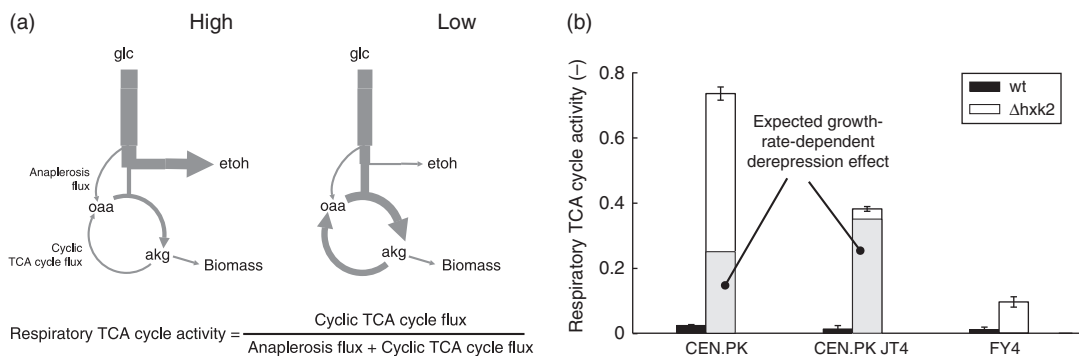


Fig. 1. Respiratory TCA cycle activities. (a) Scheme of metabolic fluxes for high and low glucose repression. Under high glucose repression (left) most of the flux through glycolysis is directed to ethanol excretion. Therefore, the respiratory TCA cycle activity as determined by the displayed equation is low. In contrast, a less glucose-repressed metabolism (right) is characterized by a higher respiratory TCA cycle activity as a higher fraction of the glycolytic flux is directed to the cyclic TCA cycle flux. Glc, glucose; etoh, ethanol; oaa, oxaloacetate; akg, α -ketoglutarate. (b) Respiratory TCA cycle activities in the different strains as determined in ^{13}C -labeling experiments from absolute flux values. The gray parts of the bars for the $\Delta hvk2$ mutants of the CEN.PK strains indicate the increase in respiratory TCA cycle activity that is related to the growth rate reduction caused by the gene deletion (as determined from Blank & Sauer, 2004).

respiring, glucose-limited cultures (van Dijken *et al.*, 2000). This finding can be further substantiated by the pronounced effect on the respiratory TCA cycle activity, which increases from $0.024 (\pm 0.003)$ to a high value of $0.735 (\pm 0.020)$ in the HXK2 deletion mutant (c.f. Fig. 1b). This increase, however, is at least partially caused by the reduction of the growth rate provoked by the mutation. In CEN.PK, Blank & Sauer (2004) demonstrated that the respiratory TCA cycle activity inversely correlates with growth rate. Nevertheless, even after correcting for the growth rate-related increase of the respiratory TCA cycle activity, a large portion of the observed increase in the HXK2 deletion mutant can still be attributed to the HXK2 deletion itself (Fig. 1b).

In contrast, the FY4 $\Delta hvk2$ strain behaves almost the same as the corresponding parent strain, with an almost identical growth rate (0.32 h^{-1}), identical biomass yield ($0.16 \text{ g}_{\text{DW}} \text{ g}_{\text{glucose}}^{-1}$) and significantly repressed respiratory TCA cycle activity (Fig. 1b). A second independently generated HXK2 deletion in FY4 and in an FY4-related strain (YSBN6) confirmed that HXK2 deletion in the FY4 strain indeed has basically no effect on the physiology (c.f. Supporting Information).

In JT4, the HXK2 deletion results in a very small relaxation from glucose repression but not to the same extent as in the CEN.PK strain (biomass yield $0.19 \text{ g}_{\text{DW}} \text{ g}_{\text{glucose}}^{-1}$ in JT4 $\Delta hvk2$; c.f. Fig. 1 for the respiratory TCA cycle activity). As in CEN.PK, the HXK2 deletion in JT4 also causes a drastic reduction of the growth rate (0.17 h^{-1}). The comparison of CEN.PK $\Delta hvk2$ and JT4 $\Delta hvk2$, where the only difference is the repaired point mutation, demonstrates that the adenylate cyclase-mediated PKA pathway restores the physiological state of glucose repression in JT4 $\Delta hvk2$, but not the growth rate.

Overall, these findings indicate that in CEN.PK, Hxk2 has an exclusive role for realizing the physiological state of glucose repression, whereas 'backup' systems for glucose repression must exist in JT4 and FY4. The question is whether the FY4 strain upon HXK2 deletion also draws on the PKA pathway to maintain glucose repression on a physiological level. Alternatively, Hxk1 could also act as backup system or it is also possible that Hxk1 is already active in FY4 in the first place. To answer this question, we performed an in-depth omics analysis of the wild-type parent strains. Using state of the art proteomics (Lange

et al., 2008) and metabolomics (Ewald *et al.*, 2009) techniques we determined the absolute amounts of 36 intracellular metabolites from central metabolism and the concentrations of 84 enzymes relative to an internal standard.

Omics comparison

On the metabolome level, the CEN.PK and the JT4 strains are very similar. However, we found significant differences between the CEN.PK/JT4 strains and the FY4 strain (Fig. 2; Table S2). In particular, the metabolites in the upper glycolysis and the pentose phosphate pathway exhibit higher concentrations in the CEN.PK (on average twofold). The metabolite data from TCA cycle intermediates indicate different substrate-to-product ratios in this part of the metabolic network (c.f. Fig. S1). In particular, several reactions (such as those catalyzed by enolase, isocitrate dehydrogenase, and succinate dehydrogenase), which are known to be influenced by glucose repression (Schuurmans *et al.*, 2008), are further shifted from equilibrium (c.f. Fig. S1), indicating a lower catalytic capacity for these reactions (Kümmel *et al.*, 2006).

The proteome data also revealed that the CEN.PK and JT4 strains are almost identical, whereas significant differences exist between the CEN.PK/JT4 strains and the FY4 strain (Fig. 3; Table S3). In general, the CEN.PK/JT4 strains have lower protein levels than the FY4 strain. In different parts of the central metabolic network, proteins were identified that are more than eightfold less abundant in

CEN.PK/JT4 compared with FY4; for example the hexokinase 1 (Hxk1), the α -ketoglutarate dehydrogenase (Kgd1), and the α,α -trehalose-phosphate synthase (Tsl1). As a general trend, proteins with a lower abundance in CEN.PK/JT4 are proteins known to be glucose repressed (i.e. Hxk1, Glk1, Tdh1, Eno1, Pyk2, and Ald4) (Navarro-Avino *et al.*, 1999; Rodriguez *et al.*, 2001; Schuurmans *et al.*, 2008). In fact, many of the less abundant proteins in CEN.PK have been shown to be transcriptionally upregulated upon deletion of HXK2 (Westergaard *et al.*, 2007).

Differential TF activity

In a statistical enrichment analysis of the proteome data we asked which TFs could have caused the differential protein expression patterns (see Materials and methods for details). This analysis revealed that the activities of the TFs Mig1, Nrg1, and Nrg2 are likely more active in CEN.PK (TF *P*-value < 0.02). These repressors – known to be involved in glucose repression (Horak *et al.*, 2002) – are all downstream of Snf1, suggesting a lower Snf1 activity in CEN.PK. The enrichment analysis further suggested the two TFs Msn2 and Msn4 to be less active in CEN.PK (*P*-values < 0.002). In addition to these activators' involvement in the general stress response, they are also known to mediate hyperosmotic shock resistance (Martinez-Pastor *et al.*, 1996). In fact, we found that CEN.PK is much less resistant to hyperosmotic stress, as no CEN.PK cells survived 40 min in a high osmolar glycerol solution, whereas the survival rate

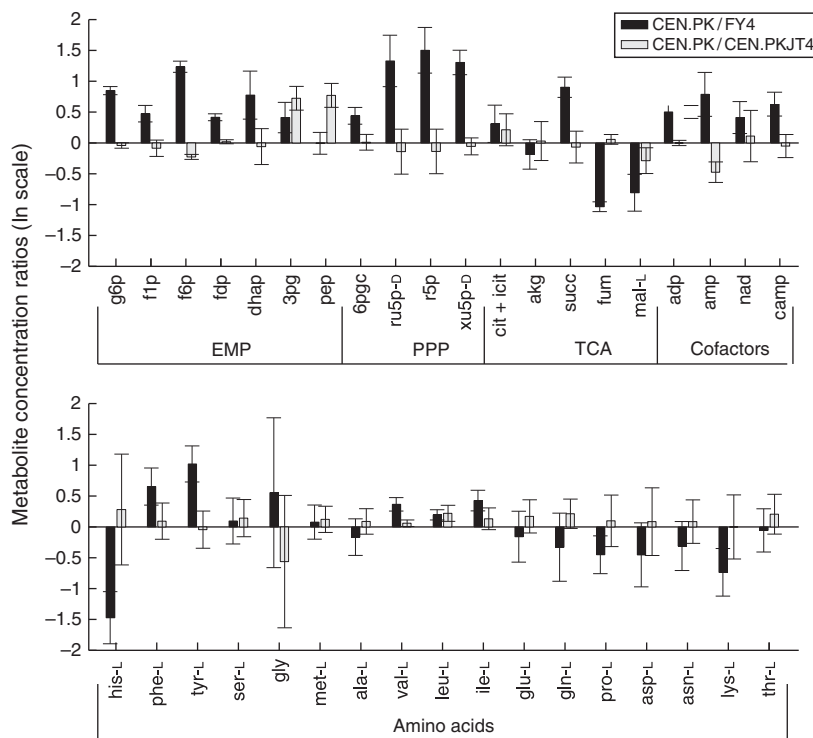
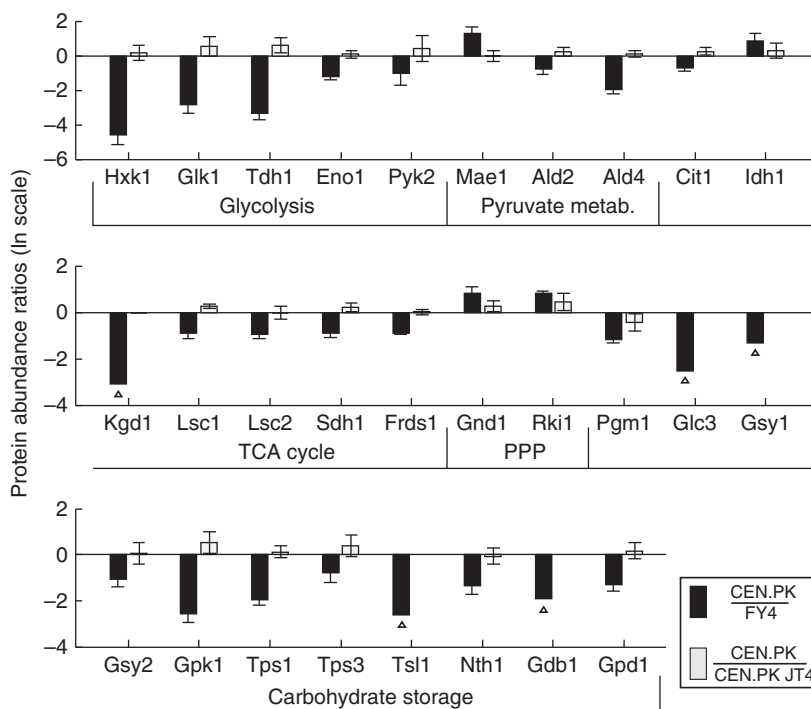


Fig. 2. Metabolite concentration differences in CEN.PK in comparison with FY4 and CEN.PK JT4. The natural logarithms of the concentration ratio of CEN.PK and CEN.PK JT4 vs. FY4 are displayed. Negative numbers correspond to lower concentrations in CEN.PK and CEN.PK JT4. Error bars indicate the SD. Metabolite concentrations were determined via GC-TOF (TCA cycle intermediates and amino acids) or LC-MS/MS (Embsden-Meyerhoff and PP pathway intermediates and cofactors) in biological duplicates. g6p, glucose 6-phosphate; f1p, fructose 1-phosphate; f6p, fructose 6-phosphate; f6p, fructose 6-phosphate; dhap, dihydroxyacetonephosphate; 3pg, 3-phosphoglycerate; pep, phosphoenolpyruvate; 6pgc, 6-phosphogluconate; ru5p-d, D-ribulose 5-phosphate; r5p, ribose 5-phosphate; xu5p-d, D-xylulose 5-phosphate; cit, citrate; icit, isocitrate; agk, α -ketoglutarate; succ, succinate; fum, fumarate; mal-L, L-malate; adp, diphosphate; amp, adenosine monophosphate; nad, nicotinamide adenine dinucleotide (reduced form).

Fig. 3. Protein concentration differences in CEN.PK in comparison with FY4 and CEN.PK JT4. The natural logarithms of the concentration ratio of CEN.PK and CE.PK JT4 vs. FY4 are displayed. Negative numbers correspond to lower concentrations in CEN.PK and CEN.PK JT4. Error bars indicate the SD. Proteins are displayed that are more than twofold more or less abundant in CEN.PK in comparison with either FY4 or CEN.PK JT4. Protein concentrations were determined via LC-S/MRM in relation to an internal standard in biological duplicates. Proteins are labeled by the corresponding gene names. Triangles indicate minimal absolute concentration ratios.



was 16% (\pm 7%) for FY4. Stress resistance is known to be repressed by high PKA activity (Thevelein & de Winde, 1999), and as Msn2 was shown to be inversely correlated with cAMP levels and PKA activity (Gorner *et al.*, 1998) this suggests that CEN.PK has a higher PKA activity than FY4.

Differential cAMP concentrations

As a proxy for PKA activity, we determined the cAMP concentrations in the three wild-type strains and the corresponding HXK2 deletion strains. We found that the CEN.PK and JT4 strains have an approximately twofold higher cAMP level than the FY4 strain (Fig. 4), potentially causing the higher basal PKA activity in these strains that was inferred from the above analysis. Whereas the HXK2 deletion strains of CEN.PK and FY4 exhibit similar cAMP levels to the corresponding parent strains, the cAMP level in the JT4 Δ hxx2 strain was found to be significantly higher than in its parent strain – likely resulting in an increased PKA activity.

Discussion

We found that CEN.PK and JT4 are virtually identical on all levels under high glucose conditions. These two strains, however, are very different compared with the FY4 strain. We found much higher metabolic rates in the CEN.PK strains, whereas the relative intracellular flux distribution is identical in both strain families. The higher metabolic rates in the CEN.PK strain might be facilitated by an increased glucose uptake/glucose phosphorylation.

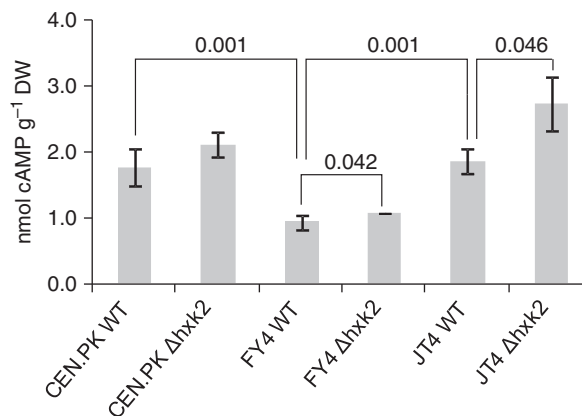


Fig. 4. cAMP concentrations in the different strains. Probability associated with a Student's paired *t*-test using a two-tailed distribution with homoscedastic variance; only *P*-values below 0.05 are shown.

Despite the increased metabolic rates, the CEN.PK strains exhibit lower expression levels of many (known glucose repressed) enzymes. As identified by the statistical enrichment analysis, the differential protein expression pattern points to differential activity of the repressors Mig1, Nrg1, and Nrg2, which are targets of the kinase Snf1, one of the key regulators for glucose repression (Santangelo, 2006). Such an increased glucose repression on the protein level invoked by the Hxk2/Snf1-pathway might be the result of the higher glycolytic fluxes in the CEN.PK strains, as glycolytic flux was found to correlate with the degree of glucose repression

(Elbing *et al.*, 2004; Otterstedt *et al.*, 2004). As we found practically identical Hxk2 expression levels in both strains (CEN.PK/FY4 = 1.24 ± 0.21 ; c.f. Table S3) and also identical HXK2 amino acid sequences, the increased Hxk2 activity (i.e. the decreased Snf1 activity) in CEN.PK compared with FY4 is not due to different Hxk2 sequences or expression levels.

The decreased Snf1 activity in CEN.PK could also be caused by such increased PKA activity, as PKA might have the potential to inactivate Snf1 activity (Haurie *et al.*, 2004; Hedbacker *et al.*, 2004; Slattery *et al.*, 2008). Indeed, our experiments suggested a higher basal PKA activity in the CEN.PK strains. As the JT4 strain was found to be identical to the CEN.PK strain on all levels, the point mutation has obviously no effect in the wild-type CEN.PK. Hence, this mutation cannot be the reason for the observed differences in the CEN.PK and FY4 proteomes and metabolomes, which are likely rather a result of the differential Snf1 and PKA activity.

The different physiological responses upon the HXK2 deletion in the CEN.PK and JT4 strains indicate that an intact CYR1 is able to partly maintain glucose repression on the physiological level in an HXK2 deletion background. Indeed, the JT4 Δ hxc2 strain likely has an increased PKA activity compared with JT4, as indicated by a significantly higher cAMP concentration in JT4 Δ hxc2. In fact, a role for cAMP/PKA in catabolite repression was suggested earlier (Eraso & Gancedo, 1984; Thompson-Jaeger *et al.*, 1991).

Finally, we are still left with the question why CEN.PK and FY4 respond so differently on the physiological level to an HXK2 deletion. Polymorphism in the CYR1 can be excluded for two reasons: (1) repairing the CYR1 defect in CEN.PK Δ hxc2 restores the physiological repression state but not the drop in the growth rate, and in FY4 Δ hxc2 growth rate is also unaltered; (2) cAMP levels in FY4 and FY4 Δ hxc2 are identical, indicating unaltered PKA activity in these two strains. (In contrast, we found increased cAMP levels in JT4 Δ hxc2 compared with JT4, pointing to an increased PKA activity in the HXK2 deletion strain.) Thus, we hypothesize that in FY4 Hxk1 might be used a backup to (1) maintain a high glycolytic flux and to (2) sustain a Hxk(1/2)/Snf1-dependent glucose repression. This might not be possible in CEN.PK.

Conclusion

This paper reports a comparative multiomic analysis of two important and commonly used yeast strains and a variant of one of them under high glucose conditions. We found significant differences in the metabolome, proteome and physiology of the two investigated yeast strain families and in the way these strains realize glucose repression on the physiological level. Further, we generated novel evidence on

the overlap between the classical glucose repression pathway and the glucose-activated cAMP/PKA signaling pathway. The identified strain differences highlight the effects of genetic backgrounds on major metabolic pathways such as those involved in glucose signaling and regulation. Although this unbiased comparison does not comprehensively answer all questions, it represents a starting point for further analysis that will likely reveal additional mechanisms involved in the phenomena reported. Nevertheless, the results of our comparative study with two commonly used yeast strain families – performed with identical analytical platforms and identical conditions – will presumably have the potential to resolve some conflicting findings that exist in the field, or at least provide possible explanations for unexplainable or unexpected observations.

Acknowledgements

We thank Jack Pronk for providing the strain CEN.PK JT4 and Stephanie Heux for generating the HXK2 deletion mutant of this strain. Furthermore, we thank Reinhard Dechant for helpful discussions and Dirk Müller for critical reading of an earlier version of this manuscript. Financial support from the Swiss initiative in systems biology, SystemsX.ch, within the project YeastX is gratefully acknowledged.

References

- Ahuatzi D, Herrero P, de la Cera T & Moreno F (2004) The glucose-regulated nuclear localization of hexokinase 2 in *Saccharomyces cerevisiae* is Mig1-dependent. *J Biol Chem* **279**: 14440–14446.
- Ahuatzi D, Riera A, Pelaez R, Herrero P & Moreno F (2007) Hxk2 regulates the phosphorylation state of Mig1 and therefore its nucleocytoplasmic distribution. *J Biol Chem* **282**: 4485–4493.
- Beney L, Marechal PA & Gervais P (2001) Coupling effects of osmotic pressure and temperature on the viability of *Saccharomyces cerevisiae*. *Appl Microbiol Biot* **56**: 513–516.
- Bisson LF & Kunathigan V (2003) On the trail of an elusive flux sensor. *Res Microbiol* **154**: 603–610.
- Blank LM & Sauer U (2004) TCA cycle activity in *Saccharomyces cerevisiae* is a function of the environmentally determined specific growth and glucose uptake rates. *Microbiology* **150**: 1085–1093.
- Boyle EI, Weng S, Gollub J, Jin H, Botstein D, Cherry JM & Sherlock G (2004) GO::TermFinder – open source software for accessing Gene Ontology information and finding significantly enriched Gene Ontology terms associated with a list of genes. *Bioinformatics* **20**: 3710–3715.
- Brachmann CB, Davies A, Cost GJ, Caputo E, Li J, Hieter P & Boeke JD (1998) Designer deletion strains derived from *Saccharomyces cerevisiae* S288C: a useful set of strains and

- plasmids for PCR-mediated gene disruption and other applications. *Yeast* **14**: 115–132.
- Carlson M (1999) Glucose repression in yeast. *Curr Opin Microbiol* **2**: 202–207.
- de Koning W & van Dam K (1992) A method for the determination of changes of glycolytic metabolites in yeast on a subsecond time scale using extraction at neutral pH. *Anal Biochem* **204**: 118–123.
- de la Cera T, Herrero P, Moreno-Herrero F, Chaves RS & Moreno F (2002) Mediator factor Med8p interacts with the hexokinase 2: implication in the glucose signalling pathway of *Saccharomyces cerevisiae*. *J Mol Biol* **319**: 703–714.
- De Winde JH, Crauwels M, Hohmann S, Thevelein JM & Winderickx J (1996) Differential requirement of the yeast sugar kinases for sugar sensing in establishing the catabolite-repressed state. *Eur J Biochem* **241**: 633–643.
- Elbing K, Larsson C, Bill RM *et al.* (2004) Role of hexose transport in control of glycolytic flux in *Saccharomyces cerevisiae*. *Appl Environ Microb* **70**: 5323–5330.
- Entian KD (1980) Genetic and biochemical evidence for hexokinase PII as a key enzyme involved in carbon catabolite repression in yeast. *Mol Gen Genet* **178**: 633–637.
- Eraso P & Gancedo JM (1984) Catabolite repression in yeasts is not associated with low levels of cAMP. *Eur J Biochem* **141**: 195–198.
- Ewald JC, Heux S & Zamboni N (2009) High-throughput quantitative metabolomics: workflow for cultivation, quenching, and analysis of yeast in a multiwell format. *Anal Chem* **81**: 3623–3629.
- Fischer E, Zamboni N & Sauer U (2004) High-throughput metabolic flux analysis based on gas chromatography-mass spectrometry derived ¹³C constraints. *Anal Biochem* **325**: 308–316.
- Gancedo JM (1998) Yeast carbon catabolite repression. *Microbiol Mol Biol R* **62**: 334–361.
- Gonzalez B, Francois J & Renaud M (1997) A rapid and reliable method for metabolite extraction in yeast using boiling buffered ethanol. *Yeast* **13**: 1347–1355.
- Gorner W, Durchschlag E, Martinez-Pastor MT *et al.* (1998) Nuclear localization of the C2H2 zinc finger protein Msn2p is regulated by stress and protein kinase A activity. *Gene Dev* **12**: 586–597.
- Guldener U, Heck S, Fielder T, Beinbauer J & Hegemann JH (1996) A new efficient gene disruption cassette for repeated use in budding yeast. *Nucleic Acids Res* **24**: 2519–2524.
- Haurie V, Sagliocco F & Boucherie H (2004) Dissecting regulatory networks by means of two-dimensional gel electrophoresis: application to the study of the diauxic shift in the yeast *Saccharomyces cerevisiae*. *Proteomics* **4**: 364–373.
- Hedbacker K, Townley R & Carlson M (2004) Cyclic AMP-dependent protein kinase regulates the subcellular localization of Snf1–Sip1 protein kinase. *Mol Cell Biol* **24**: 1836–1843.
- Horak J, Regelmann J & Wolf DH (2002) Two distinct proteolytic systems responsible for glucose-induced degradation of fructose-1,6-bisphosphatase and the Gal2p transporter in the yeast *Saccharomyces cerevisiae* share the same protein components of the glucose signaling pathway. *J Biol Chem* **277**: 8248–8254.
- Jiang H, Medintz I, Zhang B & Michels CA (2000) Metabolic signals trigger glucose-induced inactivation of maltose permease in *Saccharomyces*. *J Bacteriol* **182**: 647–654.
- Johnston M & Kim JH (2005) Glucose as a hormone: receptor-mediated glucose sensing in the yeast *Saccharomyces cerevisiae*. *Biochem Soc T* **33**: 247–252.
- King NL, Deutsch EW, Ranish JA *et al.* (2006) Analysis of the *Saccharomyces cerevisiae* proteome with PeptideAtlas. *Genome Biol* **7**: R106.
- Kümmel A, Panke S & Heinemann M (2006) Putative regulatory sites unraveled by network-embedded thermodynamic analysis of metabolome data. *Mol Syst Biol* **2**: 2006.0034.
- Lange V, Malmstrom JA, Didion J *et al.* (2008) Targeted quantitative analysis of *Streptococcus pyogenes* virulence factors by multiple reaction monitoring. *Mol Cell Proteomics* **7**: 1489–1500.
- Luo B, Groenke K, Takors R, Wandrey C & Oldiges M (2007) Simultaneous determination of multiple intracellular metabolites in glycolysis, pentose phosphate pathway and tricarboxylic acid cycle by liquid chromatography-mass spectrometry. *J Chromatogr A* **1147**: 153–164.
- Ma H & Botstein D (1986) Effects of null mutations in the hexokinase genes of *Saccharomyces cerevisiae* on catabolite repression. *Mol Cell Biol* **6**: 4046–4052.
- Mallick P, Schirle M, Chen SS *et al.* (2007) Computational prediction of proteotypic peptides for quantitative proteomics. *Nat Biotechnol* **25**: 125–131.
- Martinez-Pastor MT, Marchler G, Schuller C, Marchler-Bauer A, Ruis H & Estruch F (1996) The *Saccharomyces cerevisiae* zinc finger proteins Msn2p and Msn4p are required for transcriptional induction through the stress response element (STRE). *EMBO J* **15**: 2227–2235.
- Mbonyi K, van Aelst L, Arguelles JC, Jans AW & Thevelein JM (1990) Glucose-induced hyperaccumulation of cyclic AMP and defective glucose repression in yeast strains with reduced activity of cyclic AMP-dependent protein kinase. *Mol Cell Biol* **10**: 4518–4523.
- Navarro-Avino JP, Prasad R, Miralles VJ, Benito RM & Serrano R (1999) A proposal for nomenclature of aldehyde dehydrogenases in *Saccharomyces cerevisiae* and characterization of the stress-inducible ALD2 and ALD3 genes. *Yeast* **15**: 829–842.
- Otterstedt K, Larsson C, Bill RM, Stahlberg A, Boles E, Hohmann S & Gustafsson L (2004) Switching the mode of metabolism in the yeast *Saccharomyces cerevisiae*. *EMBO Rep* **5**: 532–537.
- Picotti P, Lam H, Campbell D *et al.* (2008) A database of mass spectrometric assays for the yeast proteome. *Nat Methods* **5**: 913–914.
- Randez-Gil F, Sanz P, Entian KD & Prieto JA (1998) Carbon source-dependent phosphorylation of hexokinase PII and its role in the glucose-signaling response in yeast. *Mol Cell Biol* **18**: 2940–2948.

- Rodriguez A, De La Cera T, Herrero P & Moreno F (2001) The hexokinase 2 protein regulates the expression of the GLK1, HXK1 and HXK2 genes of *Saccharomyces cerevisiae*. *Biochem J* **355**: 625–631.
- Rolland F, Winderickx J & Thevelein JM (2002) Glucose-sensing and -signalling mechanisms in yeast. *FEMS Yeast Res* **2**: 183–201.
- Rose M, Albig W & Entian KD (1991) Glucose repression in *Saccharomyces cerevisiae* is directly associated with hexose phosphorylation by hexokinases PI and PII. *Eur J Biochem* **199**: 511–518.
- Santangelo GM (2006) Glucose signaling in *Saccharomyces cerevisiae*. *Microbiol Mol Biol R* **70**: 253–282.
- Schacherer J, Ruderfer DM, Gresham D, Dolinski K, Botstein D & Kruglyak L (2007) Genome-wide analysis of nucleotide-level variation in commonly used *Saccharomyces cerevisiae* strains. *PLoS One* **2**: e322.
- Schuermans JM, Boorsma A, Lascaris R, Hellingwerf KJ & Teixeira de Mattos MJ (2008) Physiological and transcriptional characterization of *Saccharomyces cerevisiae* strains with modified expression of catabolic regulators. *FEMS Yeast Res* **8**: 26–34.
- Slattery MG, Liko D & Heideman W (2008) Protein kinase A, TOR, and glucose transport control the response to nutrient depletion in *Saccharomyces cerevisiae*. *Eukaryot Cell* **7**: 358–367.
- Teixeira MC, Monteiro P, Jain P et al. (2006) The YEASTRACT database: a tool for the analysis of transcription regulatory associations in *Saccharomyces cerevisiae*. *Nucleic Acids Res* **34**: D446–D451.
- Tettelin H, Agostoni Carbone ML, Albermann K et al. (1997) The nucleotide sequence of *Saccharomyces cerevisiae* chromosome VII. *Nature* **387**: 81–84.
- Thevelein JM & de Winde JH (1999) Novel sensing mechanisms and targets for the cAMP-protein kinase A pathway in the yeast *Saccharomyces cerevisiae*. *Mol Microbiol* **33**: 904–918.
- Thompson-Jaeger S, Francois J, Gaughran JP & Tatchell K (1991) Deletion of SNF1 affects the nutrient response of yeast and resembles mutations which activate the adenylate cyclase pathway. *Genetics* **129**: 697–706.
- van Dijken JP, Bauer J, Brambilla L et al. (2000) An interlaboratory comparison of physiological and genetic properties of four *Saccharomyces cerevisiae* strains. *Enzyme Microb Tech* **26**: 706–714.
- Vanhalewyn M, Dumortier F, Debast G et al. (1999) A mutation in *Saccharomyces cerevisiae* adenylate cyclase, Cyr1K1876 M, specifically affects glucose- and acidification-induced cAMP signalling and not the basal cAMP level. *Mol Microbiol* **33**: 363–376.
- Verduyn C, Postma E, Scheffers WA & Van Dijken JP (1992) Effect of benzoic acid on metabolic fluxes in yeasts: a continuous-culture study on the regulation of respiration and alcoholic fermentation. *Yeast* **8**: 501–517.
- Westergaard SL, Oliveira AP, Bro C, Olsson L & Nielsen J (2007) A systems biology approach to study glucose repression in the yeast *Saccharomyces cerevisiae*. *Biotechnol Bioeng* **96**: 134–145.
- Winston F, Dollard C & Ricupero-Hovasse SL (1995) Construction of a set of convenient *Saccharomyces cerevisiae* strains that are isogenic to S288C. *Yeast* **11**: 53–55.
- Zamboni N, Fischer E & Sauer U (2005) FiatFlux – a software for metabolic flux analysis from ¹³C-glucose experiments. *BMC Bioinformatics* **6**: 209.
- Zaragoza O, Lindley C & Gancedo JM (1999) Cyclic AMP can decrease expression of genes subject to catabolite repression in *Saccharomyces cerevisiae*. *J Bacteriol* **181**: 2640–2642.
- Zimmermann FK & Scheel I (1977) Mutants of *Saccharomyces cerevisiae* resistant to carbon catabolite repression. *Mol Gen Genet* **154**: 75–82.

Supporting Information

Additional Supporting Information may be found in the online version of this article:

Table S1. TFs that are potentially differently active in CEN.PK and FY4.

Table S2. Measured metabolite concentrations.

Table S3. The 84 measured protein concentration differences.

Table S4. Physiological parameters of aerobic glucose-growing batch cultures in ¹³C-labeling experiments performed in deep well plates.

Fig. S1. Substrate-to-product ratio differences in CEN.PK in comparison with FY4 and CEN.PK JT4 and the ratios of the corresponding enzyme amounts.

Appendix S1. Validation of the physiological phenotype of the HXK2 deletion in FY4.

Please note: Wiley-Blackwell is not responsible for the content or functionality of any supporting materials supplied by the authors. Any queries (other than missing material) should be directed to the corresponding author for the article.